

A rational design of bimetallic PdAu nanoflowers as efficient catalysts for methanol oxidation reaction

Jinyang Liu(刘锦阳), Min Wu(武敏), Xinyi Yang(杨新一), Juan Ding(丁娟), Weiwei Lei(类伟巍), Yongming Sui(隋永明)

Citation: Chin. Phys. B, 2021, 30 (**5**): 056102. DOI: 10.1088/1674-1056/abda2f
Journal homepage: http://cpb.iphy.ac.cn; http://iopscience.iop.org/cpb

What follows is a list of articles you may be interested in

Anti-oxidation characteristics of Cr-coating on surface of Ti-45Al-8.5Nb alloy by plasma surface metallurgy technique

Bing Zhou(周兵), Ya-Rong Wang(王亚榕), Ke Zheng(郑可), Yong Ma(马永), Yong-Sheng Wang(王永胜), Sheng-Wang Yu(于盛旺), and Yu-Cheng Wu(吴玉程)

Chin. Phys. B, 2020, 29 (**12**): 126101. DOI: 10.1088/1674-1056/aba9c2

Effects of Re, Ta, and W in [110] (001) dislocation core of *γ*/*γ*' interface to Ni-based superalloys: First-principles study

Chuanxi Zhu(朱传喜), Tao Yu(于涛)

Chin. Phys. B, 2020, 29 (**9**): 096101. DOI: 10.1088/1674-1056/abad26

Composition effect on elastic properties of model NiCo-based superalloys

Weijie Li(李伟节), Chongyu Wang(王崇愚)

Chin. Phys. B, 2020, 29 (**2**): 026102. DOI: 10.1088/1674-1056/ab6204

First-principles studies on carbon diffusion in tungsten

Chi Song(宋驰), Xiang-Shan Kong(孔祥山), C S Liu(刘长松)

Chin. Phys. B, 2019, 28 (**11**): 116106. DOI: 10.1088/1674-1056/ab4bb9

Effects of temperature and point defects on the stability of C15 Laves phase in iron: A molecular dynamics investigation

Hao Wang(王昊), Ning Gao(高宁), Guang-Hong Lü(吕广宏), Zhong-Wen Yao(姚仲文)

Chin. Phys. B, 2018, 27 (**6**): 066104. DOI: 10.1088/1674-1056/27/6/066104

A rational design of bimetallic PdAu nanoflowers as efficient catalysts for methanol oxidation reaction*

Jinyang Liu(刘锦阳)[1], Min Wu(武敏)[1], Xinyi Yang(杨新一)[1,†], Juan Ding(丁娟)[2,‡], Weiwei Lei(类伟巍)[3], and Yongming Sui(隋永明)[1]

[1] *State Key Laboratory of Superhard Materials, College of Physics, Jilin University, Changchun* 130012, *China*
[2] *Zhuhai College, Jilin University, Zhuhai* 519041, *China*
[3] *Institute for Frontier Materials, Deakin University, Geelong, Victoria,* 3216, *Australia*

(Received 11 December 2020; revised manuscript received 30 December 2020; accepted manuscript online 11 January 2021)

Methanol fuel cells have been intensively developed as clean and high-efficiency energy conversion system due to their high efficiency and low emission of pollutants. Here, we developed a simple aqueous synthetic method to prepare bimetallic PdAu nanoflowers catalysts for methanol oxidation reaction (MOR) in alkaline environment. Their composition can be directly tuned by changing the ratio between Pd and Au precursors. Compared with commercial Pd/C catalyst, all of the PdAu nanoflowers catalysts show the enhanced catalytic activity and durability. In particular, the PdAu nanoflowers specific activity reached 0.72 mA/cm^2, which is 14 times that of commercial Pd/C catalyst. The superior MOR activity could be attributed to the unique porous structure and the shift of the d-band center of Pd.

Keywords: PdAu alloy, methanol oxidation reaction, catalyst

PACS: 61.82.Bg, 88.30.pf, 82.45.Jn **DOI:** 10.1088/1674-1056/abda2f

1. Introduction

Direct methanol fuel cell (DMFC), which is an emerging energy for portable and transport applications, has attracted much attention due to its high energy density and environmentally friendly.[1] Pt and Pt-based catalysts as the best catalysts have been widely applied in the methanol oxidation reaction (MOR) that is the anodic reaction of DMFC.[2] However, Pt and Pt-based catalysts are not only high cost but also easily poisoned by CO[3] which is generated in catalytic processes. Pd and Pd-based catalysts as a replacement attract more and more attention because of their low price.[4] And recent research, which could be a strong reason to explore Pd and Pd-based catalysts, shows that there is no evidence of CO formation for Pd-based catalysts in an alkaline environment.[5]

There are two ways to synthesize nanocatalysts with a high catalytic performance. One way is based on bifunctional reaction mechanism[6] and surface ligand effect.[7] In this way, one metal is doped with another metal like noble metal (Au,[8] Pt,[9] and Ru[10]) or transition metal (Ni,[11] Co,[12] and Cu[13]). Enhancement of the catalytic activity can attribute to the addition of different metal, which causes the shift of the d-band center of Pd with respect to the Fermi level in the alloys.[14] The other way is shape-controlled metal nanocrystals, such as wires,[8] icosahedrons,[15] cubes,[16] rob,[17] decahedrons,[18] and dendrites.[19] All of these show a high electrocatalytic activity because of high surface-to-volume ratio, high index facets, and lattice strain effects.[20] What is more, Han *et al.*[21] and Feng *et al.*[22] reported that they integrated the ways of the above mentioned to design and prepare three-dimensional multi-element alloy catalysts with superior catalytic activity for alcohol oxidation, which supplied a new way to design nanocatalysts with a high catalytic performance. Now, some strategies have been applied to design and optimize materials with enhancing catalytic performances, including seed mediated growth,[23] chemical vapor deposition,[24] and selective etching.[25] But these methods are often complicated and time consuming, which restrict their further applications.

In this work, we propose a simple way to synthesize flower-liked bimetallic PdAu nanocatalysts with controllable Pd/Au molar ratios. The as-prepared PdAu nanoflowers are self-supported porous structures with a high surface area. Especially, all of the PdAu nanoflowers catalysts show higher catalytic activities for MOR than commercial Pd/C catalyst in an alkaline environment due to their particular porous architectures and the shift of the d-band center of Pd.

2. Experimental details

Chemical reagent Palladium (II) sodium chloride ($NaPdCl_4$), chloroauric acid ($HAuCl_4$), and polyvinyl pyrrolidone (PVP, Mw≈40000) were purchased from Sigma-Aldrich. Citric acid, ethyl alcohol absolute, methanol (CH_3OH),

*Project supported by the National Natural Science Foundation of China (Grant Nos. 118740271 and 1774124), Technology Development Program of Jilin Province, China (Grant No. 20180101285JC), and the China Postdoctoral Science Foundation (Grant Nos. 2019T120233 and 2017M621198).

†Corresponding author. E-mail: yangxinyi@jlu.edu.cn
‡Corresponding author. E-mail: juanding0127@163.com

© 2021 Chinese Physical Society and IOP Publishing Ltd

sodium hydroxide (NaOH), and sodium borohydride ($NaBH_4$) were purchased from Sinopharm Chemical Reagent Company. Nafion 117 solution (5 wt%) and commercial Pd/C were ordered from Alfa Aesar. All the chemicals and materials were used as received.

Synthesis of PdAu nanoflowers catalysts To synthesize the PdAu nanoflowers catalysts, 11 mg citric acid and 100 mg PVP were mixed with 30 mL deionized water (18.2 MΩ·cm), then it was injected with the mixture of 0.2 mM $NaPdCl_4$ (37.5 μL) and 0.24 mM $HAuCl_4$ (31 μL) under magnetic stirring. The 2.1 mg $NaBH_4$ was dissolved in 3 mL deionized water and subsequently added to the reaction mixture, followed by stirring for 30 min at room temperature. Finally, the suspensions were filtered and washed several times with deionized water and ethyl alcohol absolute to completely remove all excess reducing agent. Control experiments were performed by changing the molar ratio of $NaPdCl_4$ and $HAuCl_4$, while the other experimental conditions were remained unchanged.

3. Characterization

Materials characterization Transmission electron microscopy (TEM), STEM-element mapping, and high-resolution transmission electron microscopy (HRTEM) images of the simples were obtained on JEM2200FS with an accelerating voltage of 200 kV. X-ray diffraction was tested on Rigaku with a high-intensity microfocus rotating anode x-ray generator of MicroMax-007HF ($\lambda = 1.5418$ Å).

Electrochemical characterization All the electrochemical measurements were carried out on a three-electrode system on CHI-660E electrochemical workstation at room temperature. The sample and commercial Pd/C were applied to the surface of glassy carbon (GC) electrodes. Pt wire and saturated calomel electrode (SCE) served as the counter electrode and reference electrode, respectively. The electrochemical oxidation of methanol was performed in the mixture of 1.0 M NaOH containing 1.0 M CH_3OH solution. The electrolyte solution was deoxygenated with N_2 for 15 min before measurement.

4. Results and discussion

4.1. Characterization of Pd_1Au_1 nanoflowers catalysts

The morphology and size of Pd_1Au_1 nanoflowers catalysts were characterized by TEM. Figures 1(a) and 1(b) show the TEM images of Pd_1Au_1 nanoflowers catalysts in different magnification, whose average diameter is ca. 25 nm (insert in Fig. 1(a)). Besides, SAED pattern with obvious diffraction rings indicated its polycrystalline property. The surface structure of Pd_1Au_1 nanoflowers catalysts was characterized by HRTEM in Fig. 1(c). An individual Pd_1Au_1 catalyst displays an obvious flower shape with porous architecture assembled by staggered nanocrystals as building blocks. Constructing open porous structure is of great importance to drastically suppress the activity loss derived from the agglomeration of active sites.[26,27] The lattice spacing distance of ca. 0.227 nm can be observed clearly on the surface of Pd_1Au_1 nanoflowers catalysts, which is between the interplanar spacing value 0.224 nm of Pd (111) plane and 0.235 nm of Au (111) plane. Figure 1(d) displays the elemental mapping of Pd, Au and their overlap for the Pd_1Au_1 nanoflowers catalysts. Their overlap image can be seen clearly in elemental mapping patterns, which is a strong evidence for the generation of PdAu alloy (the signals of Pd in green and Au in yellow). And the chemical composition of Pd_1Au_1 nanoflowers catalysts is characterized by EDS analysis to be 56 : 44 (Pd : Au), which is very close to the ratio of Pd : Au. Figures 2(a) and 2(b) show the TEM of $PdAu_2$ and $PdAu_3$ nanoflowers catalysts, respectively, indicating that the morphologies of PdAu nanoflowers catalysts are independent of the molar ratio of $NaPdCl_4$ and $HAuCl_4$.

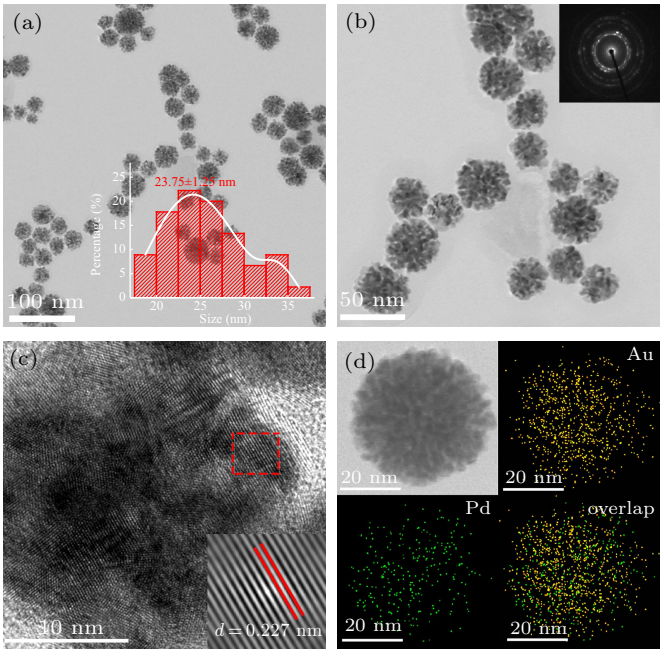


Fig. 1. (a) Low-magnification and (b) middle-magnification TEM images with SAED image of Pd_1Au_1 nanoflowers catalysts. (c) HRTEM image of Pd_1Au_1 nanoflowers catalysts. (d) HAADF-STEM-EDS mapping of Pd_1Au_1 nanoflowers catalysts.

To understand the impact of $NaBH_4$ as reductant on the growth of PdAu nanoflowers, we monitor the change of sample morphology by TEM. As shown in Fig. 3(a), a large number of dispersed nanoparticles are produced. After injecting 40 μL $NaBH_4$, both nanoparticles and nanodendrites can be simultaneously observed, indicating that branches grow from the nanoparticles (Fig. 3(b)). When injecting 100 μL $NaBH_4$, the nanodendrites begin to clump together to generate nanoflowers (Fig. 3(c)). With injecting $NaBH_4$ up to 200 μL, the nanoparticles completely form nanoflowers (Fig. 3(d)). The morphology evolution with the addition of $NaBH_4$ gives

an experimental evidence on the formation process of PdAu nanoflowers.

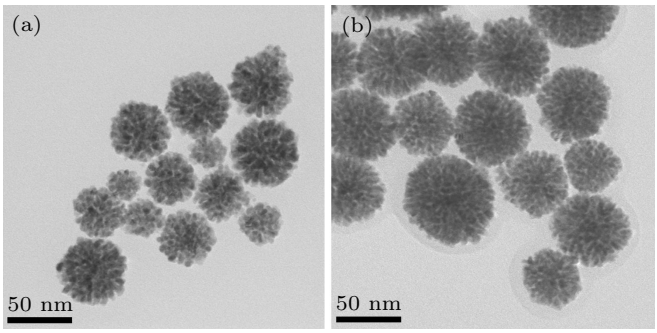


Fig. 2. The TEM of morphologies of (a) $PdAu_2$ and (b) $PdAu_3$.

Figure 4(a) shows the XRD pattern of Pd_1Au_1 nanoflowers catalysts. There are five diffraction peaks at $2\theta = 39.24°$, 45.54°, 66.46°, 79.80°, and 84.04° between monometallic Pd (JCPDS 46-1043) and Au (JCPDS 04-0784). This indicates that the products are alloy and have face-centered-cubic (fcc) structure. To more deeply investigate the surface composition and chemical state of Pd_1Au_1 nanoflowers catalysts, it is analyzed by x-ray photoelectron spectra (XPS). The high-resolution Pd 3d XPS region is shown in Fig. 4(b). Two distinct binding energies (B.E.) are 335.1 eV and 340.2 eV that correspond to Pd $3d_{5/2}$ and Pd $3d_{3/2}$, respectively. The two parts can be divided into two pairs of peaks at 335 eV, 340.15 eV, 335.95 eV, and 340.9 eV, indicating the presence of Pd^0 and Pd^{II}. Similarly, the pair of peaks located at 83.55 eV and 87.2 eV corresponding to Au $4f_{7/2}$ and Au $4f_{5/2}$ is shown in Fig. 4(c). The presence of Pd^0 and Pd^{II} is attributed to that the reduction potential of $AuCl_4^-$/Au (1.002 V) is higher than that of $PdCl_4^{2-}$/Pd (0.591 V).[28] Hence, the reduction of $AuCl_4^-$ to Au is easier than $PdCl_4^{2-}$ to Pd. Comparing with the B.E. of pure Pd (335.0 eV) and pure Au (83.8 eV), we find that the B.E. of Pd $3d_{5/2}$ for Pd_1Au_1 is higher than that of pure Pd, and the B.E. of Au $4f_{7/2}$ for Pd_1Au_1 is much lower than that of pure Au. The phenomenon can be attributed to the modification in Pd electronic structure by Au especially the d band center of Pd and intra-atomic and/or inter-atomic charge transfer between Au and Pd, when they are alloyed together in nanoflower structure.

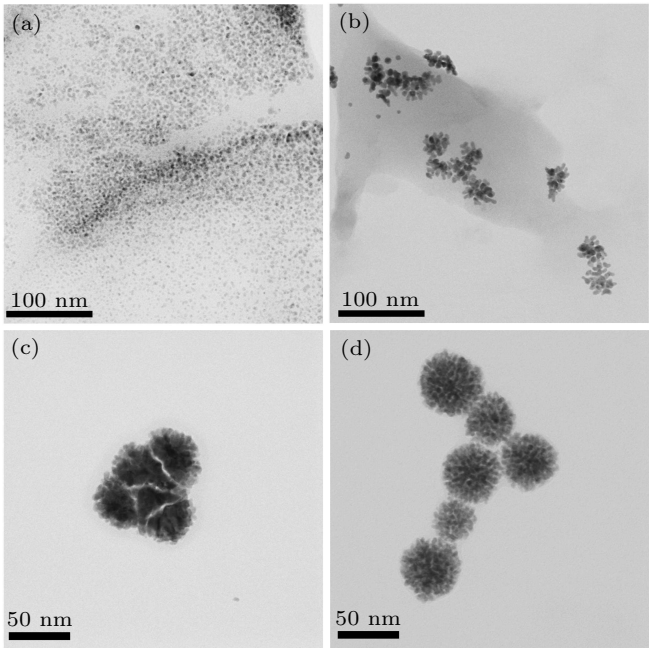


Fig. 3. TEM of morphologies of PdAu after injecting (a) 20 μL, (b) 40 μL, (c) 100 μL, and (d) 200 μL $NaBH_4$.

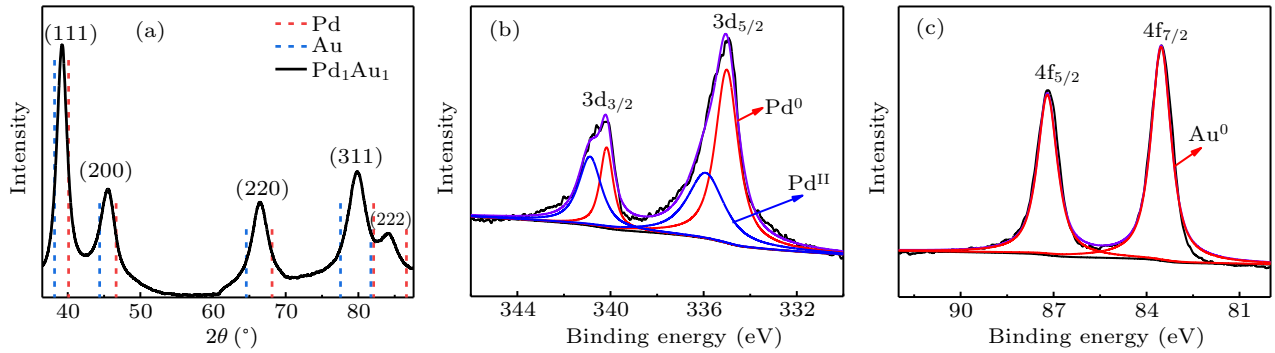


Fig. 4. (a) XRD, (b) Pd 3d XPS, and (c) Au 4f XPS spectra of Pd_1Au_1 nanoflowers catalysts.

4.2. Electrochemical properties of PdAu nanoflowers catalysts

Figure 5(a) shows the cyclic voltammograms of Pd/C, Pd_2Au, Pd_1Au_1, $PdAu_2$, and $PdAu_3$ nanoflowers catalysts measured in 1.0 M KOH solution at a scan rate of 50 mV/s. During the negative scans, the peaks locate at −0.1 V to −0.4 V can be observed for all catalysts, which are associated with the Pd oxide reduction. The peaks of Pd oxide reduction for Pd/C, Pd_2Au, Pd_1Au_1, $PdAu_2$, and $PdAu_3$ nanoflowers catalysts are located at around −0.36 V, −0.28 V, −0.26 V, −0.2 V, and −0.19 V, respectively. These peaks exhibit a shift from low potential to high potential, which is associated with decrease of Pd content in the PdAu alloy, proving that the catalytic activity of Pd is modified by Au. The electrochemical active surface area (ECSA) is calculated from the *C*–*V* curves

according to the equation ECSA $= Q/C$. In this equation, Q is the charge from integrating the peaks of Pd oxide reduction and C is 4.2 C/m^2, which is a constant charge required to reduce the monolayer of PdO adsorbed on the catalyst.

MOR activity of PdAu nanoflowers catalysts is tested in mixed solution of 1 M KOH and 1 M methanol at a scan rate of 50 mV/s. As shown in Fig. 5(b), the current density is normalized by ECSA, we can see that the C–V curves of methanol oxidation contain forward scan and backward scan. One peak located in the forward scan is associated with methanol oxidation, the other is attributed to the removal of by-production such as formate produced in forward scan. In the forward scan, the onset potential (E_0), peak potential (E_P), and peak current density (j_P) of catalysts are obtained from Fig. 5(b) and listed in Table 1. It indicates that alloying of Au with Pd can enhance the kinetics and improve the catalytic activity for methanol oxidation. The E_0 for PdAu nanoflowers catalysts is more negative than that of commercial Pd/C catalyst. With the decreasing Pd content, the E_P shifts from negative potential to positive potential and j_P first increases and then decreases. The E_P and j_P reach a maximum at PdAu (1 : 1). This phenomenon is due to that Au has insignificant electrochemical activity for methanol oxidation. Specific activity (SA) is shown in Fig. 5(c), which is calculated from the forward peak currents as normalized by ECSA. From Fig. 5(c), the Pd_1Au_1 nanoflowers catalyst has the maximum SA, which is 0.72 mA/cm^2, about 14 times that of commercial Pd/C catalyst. Others also show higher SA than commercial Pd/C catalyst. The excellent performance of PdAu nanoflowers catalysts could be attributed to the addition of Au, which makes the d-band center of Pd down shift more obviously and accelerates the reaction of methanol oxidation.

Table 1. The E_0, E_P, j_P, ECSA obtained from Fig. 3.

Catalyst	E_0 (V)	E_P (V)	j_P (mA·cm^{-2})	ECSA (cm^{-2})
Pd/C	–0.35	–0.102	0.053	1.368
Pd_2Au	–0.49	–0.116	0.691	0.142
Pd_1Au_1	–0.50	–0.118	0.721	0.118
$PdAu_2$	–0.46	–0.036	0.512	0.130
$PdAu_3$	–0.37	0.006	0.459	0.065

Since the PdAu nanoflowers catalysts have similar characteristics with other Pd and Pd-based catalysts, we compare our catalysts with some commonly reported catalysts. For example, Luo *et al.*[28] provided SA of the Pd-black catalysts, which is 0.32 mA/cm^2. Wang *et al.*[29] reported that the incorporation of Ag into Pd can enhance the MOR activity of Pd, which can be increased to 0.68 mA/cm^2 (Pd : Ag = 1 : 1) and 0.71 mA/cm^2 (Pd : Ag = 1 : 1.5). Liu *et al.*[30] showed that the porous morphology can improve the MOR specific activity of PdAu catalysts, whose best SA is 0.27 mA/cm^2. It can be seen that the Pd_1Au_1 nanoflowers catalysts are competitive and outstanding for methanol oxidation reaction compared with other catalysts.

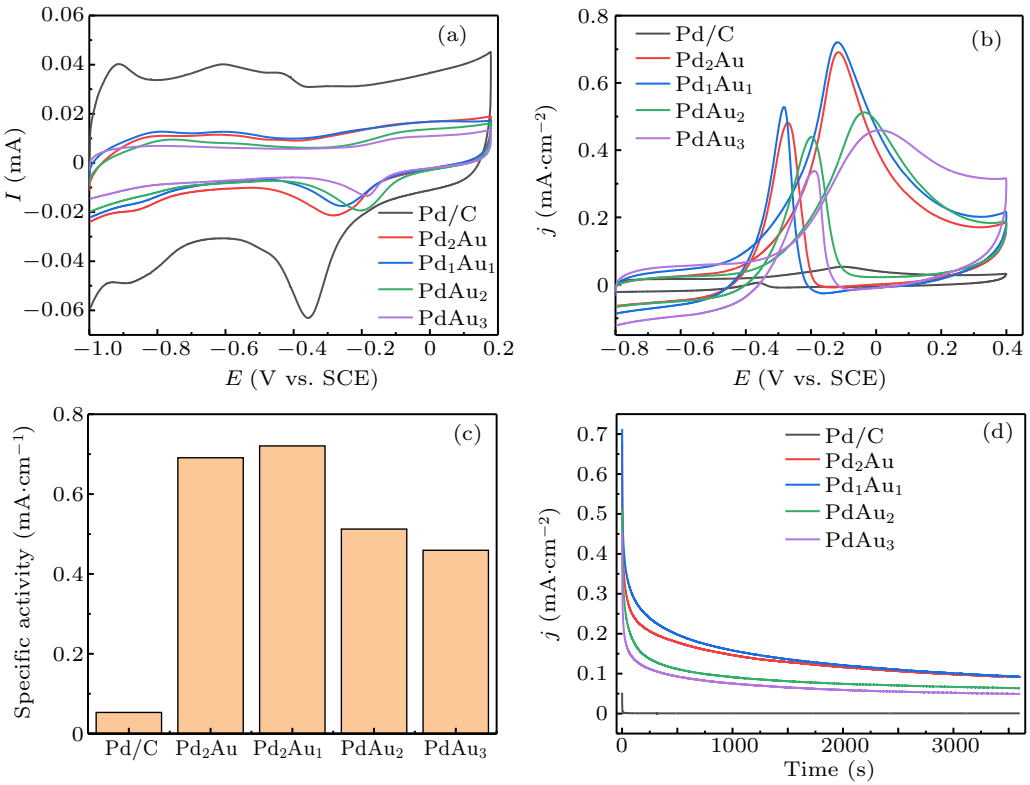


Fig. 5. Cyclic voltammograms of Pd/C, Pd_2Au, Pd_1Au_1, $PdAu_2$, and $PdAu_3$ catalysts in (a) 1 M KOH and (b) 1 M KOH+1 M CH_3OH. (c) Specific activities. (d) Chronoamperograms of Pd/C, Pd_2Au, Pd_1Au_1, $PdAu_2$, and $PdAu_3$ nanoflowers catalysts.

To evaluate the electrocatalytic endurance of PdAu nanoflowers catalysts, chronoamperometric experiment has be performed at −0.12 V and the results are shown in Fig. 5(d). All of the catalysts show a significant current decrease at first and then gradually slow down and level off. During 1 h test, all of the PdAu nanoflowers catalysts have higher current density than commercial Pd/C catalyst. And Pd_1Au_1 nanoflowers catalyst shows the highest current density at 3600 s. From Fig. 5(d), we can infer that doping Au into Pd can effectively improve the catalyst stability toward methanol oxidation. What is more, the Pd_1Au_1 nanoflowers catalyst is the most superior catalyst among the catalysts investigated, which can illustrate that the appropriate incorporation of Au into Pd can effectively promote the reduction of PdO back to Pd to improve the stability of catalyst.

5. Conclusion

In summary, we develop a simple aqueous synthetic method to prepare bimetallic PdAu alloy nanoflowers. The prepared Pd_1Au_1 nanoflowers show the best specific activity and stability toward methanol oxidation reaction, compared with other PdAu nanoflowers catalysts and commercial Pd/C catalyst. The main reason of the enhanced electrocatalytic performance is that Au could modify the d-band center of Pd. We hope that this work could be used in designing multi-component and unprecedented electrocatalysts for direct methanol fuel cells.

References

[1] Aricò A S, Srinivasan S and Antonucci V 2001 *Fuel Cells* **1** 133
[2] Iwasita T 2002 *Electrochim. Acta* **47** 3663
[3] Bai J, Xiao X, Xue Y Y, Jiang J X, Zeng J H, Li X F and Chen Y 2018 *ACS Appl. Mater. Interfaces* **10** 19755
[4] Antolini E 2009 *Energy Environ. Sci.* **2** 915
[5] Kelly C H W, Benedetti T M, Alinezhad A, Schuhmann W, Gooding J J and Tilley R D 2018 *J. Phys. Chem. C* **122** 21718
[6] Chen H, Xing Z, Zhu S, Zhang L, Chang Q, Huang J, Cai W B, Kang N, Zhong C J and Shao M 2016 *J. Power Sources* **321** 264
[7] García-Domínguez P and Nevado C 2016 *J. Am. Chem. Soc.* **138** 3266
[8] Wang Q L, Fang R, He L L, Feng J J, Yuan J and Wang A J 2016 *J. Alloys Compd.* **684** 379
[9] Kim Y, Noh Y, Lim E J, Lee S, Choi S M and Kim W B 2014 *J. Mater. Chem. A* **2** 6976
[10] Xu H, Yan B, Zhang K, Wang J, Li S, Wang C, Shiraishi Y, Du Y and Yang P 2017 *J. Colloid Interface Sci.* **505** 1
[11] Li G, Shi B, Gong Y, Zhang Y, Wang X, Guo M and Lyu X 2020 *Mater. Chem. Phys.* **243** 122570
[12] Wang X and Xia Y 2008 *Electrochem. Commun.* **10** 1644
[13] Mandal K, Bhattacharjee D, Roy P S, Bhattacharya S K and Dasgupta S 2015 *Appl. Catal. A Gen.* **492** 100
[14] Hammer B and Nørskov J K 2000 *Adv. Catal.* **45** 71
[15] Zhang L, Guo Y, Iqbal A, Li B, Deng M, Gong D, Liu W and Qin W 2017 *J. Nanoparticle Res.* **19** 150
[16] Zhu W, Kattel S, Jiao F and Chen J G 2019 *Adv. Energy Mater.* **9** 1
[17] Zhang M, Wu Y and Yu Y 2020 *Appl. Surf. Sci.* **510** 145434
[18] Wang X, Vara M, Luo M, Huang H, Ruditskiy A, Park J, Bao S, Liu J, Howe J, Chi M, Xie Z and Xia Y 2015 *J. Am. Chem. Soc.* **137** 15036
[19] Wang H, Wu M, Wang Y, Wang H, Huang X and Yang X 2019 *Chin. Phys. B* **28** 106401
[20] Xia X, Yates J L R, Jones G, Sarwar M, Harkness I and Thompsett D 2016 *J. Mater. Chem. A* **4** 15181
[21] Han Z, Wang A J, Zhang L, Wang Z G, Fang K M, Yin Z Z and Feng J J 2019 *J. Colloid Interface Sci.* **554** 512
[22] Feng Y G, Niu H J, Mei L P, Feng J J, Fang K M and Wang A J 2020 *J. Colloid Interface Sci.* **575** 425
[23] Cargnello M, Agarwal R, Klein D R, Diroll B T, Agarwal R and Murray C B 2015 *Chem. Mater.* **27** 5833
[24] Chen Z, Ren W, Gao L, Liu B, Pei S and Cheng H M 2011 *Nat. Mater.* **10** 424
[25] Lee B C, Kim M H, Chandran J, Kim S K, Shin H J and Moon S 2008 *J. Exp. Nanosci.* **3** 87
[26] Mahmoud M A, Tabor C E, El-Sayed M A, Ding Y and Zhong L W 2008 *J. Am. Chem. Soc.* **130** 4590
[27] Lim B, Jiang M, Camargo P H C, Cho E C, Tao J, Lu X, Zhu Y and Xia Y 2009 *Science* **324** 1302
[28] Luo L M, Zhang R H, Du J J, Yang F, Liu H M, Yang Y and Zhou X W 2017 *Int. J. Hydrogen Energy* **42** 16139
[29] Wang Y, Sheng Z M, Yang H, Jiang S P and Li C M 2010 *Int. J. Hydrogen Energy* **35** 10087
[30] Liu J, Wang J, Kong F, Huang T and Yu A 2016 *Catal. Commun.* **73** 22